Report No. KS-12-1 ▪ FINAL REPORT ▪ April 2012

Measurement of the Pore Size Distribution of Limestone Aggregates in Concrete Pavement Cores: Phase I

Kyle A. Riding, Ph.D., P.E.
Asad Esmaeily, Ph.D., P.E.
Mohammadreza Mirzahosseini

Kansas State University

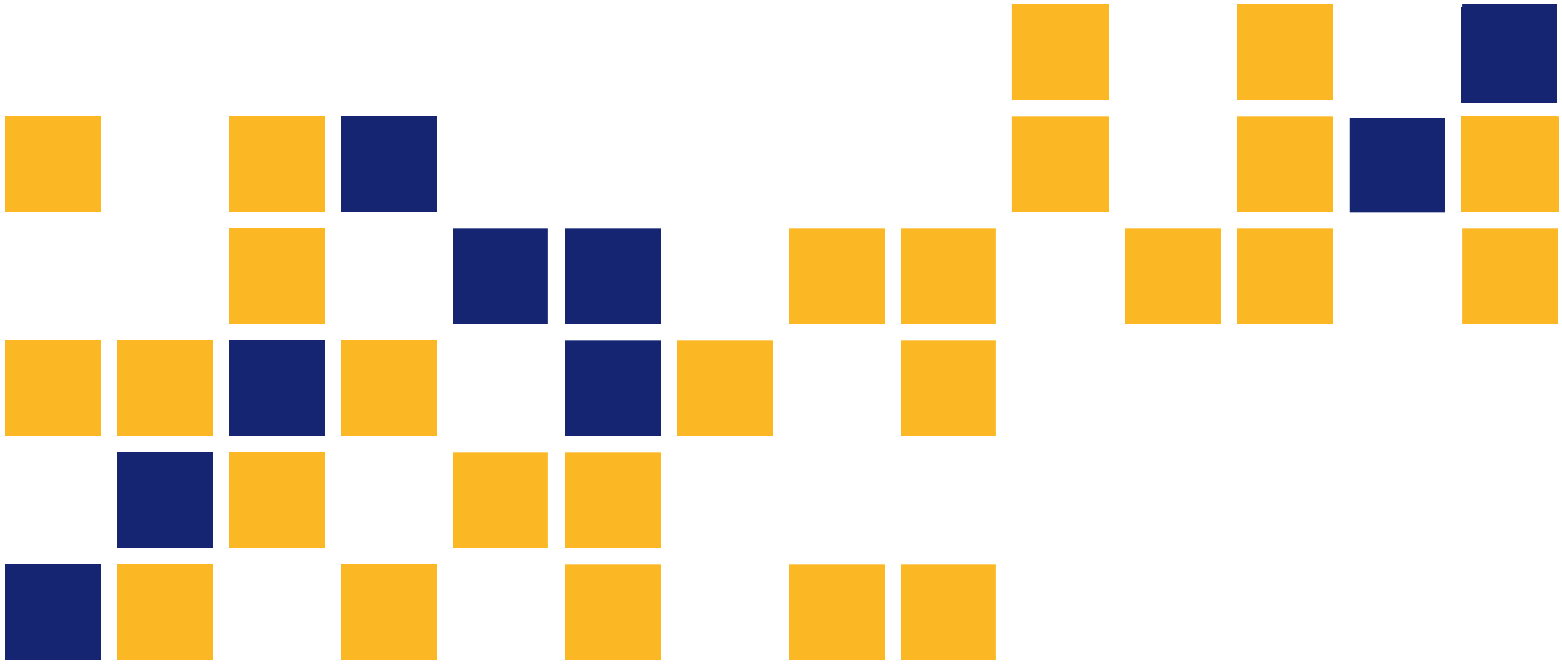

Kansas Department of Transportation

1 Report No. KS-12-1	**2 Government Accession No.**	**3 Recipient Catalog No.**
4 Title and Subtitle Measurement of the Pore Size Distribution of Limestone Aggregates in Concrete Pavement Cores: Phase I		**5 Report Date** April 2012 **6 Performing Organization Code**
7 Author(s) Kyle A. Riding, Ph.D., P.E.; Asad Esmaeily, Ph.D., P.E.; Mohammadreza Mirzahosseini		**8 Performing Organization Report No.**
9 Performing Organization Name and Address Kansas State University Department of Civil Engineering 2118 Fielder Hall Manhattan, Kansas 66506-5000		**10 Work Unit No. (TRAIS)** **11 Contract or Grant No.** C1896
12 Sponsoring Agency Name and Address Kansas Department of Transportation Bureau of Materials and Research 700 SW Harrison Street Topeka, Kansas 66603-3745		**13 Type of Report and Period Covered** Final Report April 2011–November 2011 **14 Sponsoring Agency Code** RE-0583-01
15 Supplementary Notes		

16 Abstract

Freeze-thaw damage is one of the common forms of distress for concrete pavements in Kansas. D-Cracking is a form of freeze-thaw damage caused by aggregates with poor freeze-thaw durability. It is believed that pores in the aggregates below 10 μm in diameter contribute to this poor durability. In this Phase I study, a methodology for preparing limestone coarse aggregates taken from concrete cores for examination by scanning electron microscopy (SEM) was developed. Software was developed to quantify the aggregate pore size distribution from the SEM images. The procedure was used on cores from two concrete pavements with different field performance. The aggregates from one of the pavements studied, pavement B, had a larger total area of pores and larger number of pores below 1.5 μm^2 in area. The aggregates from the other pavement, pavement A, had a smaller total area and smaller number of pores below 1.5 μm^2 in area, but a higher percentage of the pores were in this smaller pore size range. Cores from the two pavements were also tested for potential alkali-aggregate reactivity by measuring their length change after soaking in 1N NaOH solution at 80°C. It was found that the aggregates in pavement B showed much more potential for expansion from alkali-aggregate reaction than pavement A with approximately 0.2% expansion at 28 days for pavement B vs. 0.04% expansion for pavement A.

17 Key Words Concrete Pavement, Pore Size Distribution, ASR, D-Cracking, AAR		**18 Distribution Statement** No restrictions. This document is available to the public through the National Technical Information Service, Springfield, Virginia 22161	
19 Security Classification (of this report) Unclassified	**20 Security Classification (of this page)** Unclassified	**21 No. of pages** 30	**22 Price**

Form DOT F 1700.7 (8-72)

Measurement of the Pore Size Distribution of Limestone Aggregates in Concrete Pavement Cores: Phase I

Final Report

Prepared by

Kyle A. Riding, Ph.D., P.E.
Asad Esmaeily, Ph.D., P.E.
Mohammadreza Mirzahosseini

Kansas State University

A Report on Research Sponsored by

THE KANSAS DEPARTMENT OF TRANSPORTATION
TOPEKA, KANSAS

April 2012

NOTICE

The authors and the state of Kansas do not endorse products or manufacturers. Trade and manufacturers names appear herein solely because they are considered essential to the object of this report.

This information is available in alternative accessible formats. To obtain an alternative format, contact the Office of Transportation Information, Kansas Department of Transportation, 700 SW Harrison, Topeka, Kansas 66603 or phone (785) 296-3585 (Voice) (TDD).

DISCLAIMER

The contents of this report reflect the views of the authors who are responsible for the facts and accuracy of the data presented herein. The contents do not necessarily reflect the views or the policies of the state of Kansas. This report does not constitute a standard, specification or regulation.

Abstract

Freeze-thaw damage is one of the common forms of distress for concrete pavements in Kansas. D-Cracking is a form of freeze-thaw damage caused by aggregates with poor freeze-thaw durability. It is believed that pores in the aggregates below 10 μm in diameter contribute to this poor durability. In this Phase I study, a methodology for preparing limestone coarse aggregates taken from concrete cores for examination by scanning electron microscopy (SEM) was developed. Software was developed to quantify the aggregate pore size distribution from the SEM images. The procedure was used on cores from two concrete pavements with different field performance. The aggregates from one of the pavements studied, pavement B, had a larger total area of pores and larger number of pores below 1.5 μm^2 in area. The aggregates from the other pavement, pavement A, had a smaller total area and smaller number of pores below 1.5 μm^2 in area, but a higher percentage of the pores were in this smaller pore size range. Cores from the two pavements were also tested for potential alkali-aggregate reactivity by measuring their length change after soaking in 1N NaOH solution at 80°C. It was found that the aggregates in pavement B showed much more potential for expansion from alkali-aggregate reaction than pavement A with approximately 0.2% expansion at 28 days for pavement B vs. 0.04% expansion for pavement A.

Acknowledgements

The authors wish to acknowledge the financial support of the Kansas Department of Transportation (KDOT) for this research. KDOT also collected the concrete cores used in this project. Mr. Randy Billinger was the project monitor from KDOT for this project.

Table of Contents

List of Tables

Lists of Figures

Chapter 1: Introduction

1.1 Background

Recently, the Kansas Department of Transportation (KDOT) began a large study aimed at determining the efficacy of the current concrete aggregate specifications in preventing poor quality materials from being used in concrete pavements. It was found from this study that many of the concrete pavements are failing before their expected 20 year design life, even though the aggregates passed all of the current KDOT concrete aggregate specifications.

Although KDOT recognizes that damage from alkali-aggregate reaction (AAR) and D-Cracking have unique cracking patterns, damage from AAR can often resemble D-Cracking in pavements, with damage at the joints appearing first because of the increased moisture and salt availability. AAR includes both alkali-silica reaction (ASR) and alkali-carbonate reaction (ACR). Besides causing cracking, ASR can also worsen freeze-thaw damage by filling in air voids with ASR gel (Niels, Ulla Hjorth, and Boyd 1996). Kansas limestone aggregates are not required to be tested for AAR susceptibility, but may still be ASR reactive because of chert particles embedded in limestone or ACR reactive if it is a dolomitic limestone.

Freeze-thaw damage to Kansas concrete pavements can occur because of poor quality limestone aggregates. In cement paste, entrained air voids provide a location for the ice to form, preventing the expansion from occurring inside the cement paste pores. Limestone aggregates do not however contain entrained air voids that remain dry until the freezing event. In order for water to escape the aggregate and freeze inside of an entrained air void, all aggregate pores must be reasonably close to an air void. This is the reasoning behind KDOT's maximum aggregate size requirements that have helped prolong the life of some concrete pavements. Even with the smaller aggregate sizes, certain pore size distributions make it more difficult for water to escape the aggregate and reach an air void. Table 1.1 shows the size of aggregate pores found in previous studies that correlated with poor freeze-thaw resistance.

TABLE 1.1
Critical Aggregate Pore Size Ranges that Contribute to D-Cracking by Several Researchers (Pittenger and West 1995)

Study	Critical Pore Size Range
(Shakoor 1982)	0.01 μm–10 μm
(Salcedo 1984)	0.045 μm–10 μm
(Kaneuji, Winslow and Dolch 1980)	4.5 nm–5 μm
(Dubberke and Marks 1985)	0.04 μm–0.2 μm

Most quarries in Kansas operate for less than a decade before exhausting economically viable limestone beds crushed to produce aggregates. This makes it rather difficult to relate performance to new test methods or properties not measured during construction because by the time concrete pavement deterioration is noticed, the quarry that supplied the aggregate is no longer in operation to obtain virgin aggregates. This makes it necessary to examine aggregates in concrete cores taken from the pavement to determine the cause of deterioration and any contributing physical properties.

1.2 Problem Statement

This report documents Phase I of a study with the overall goal of determining if the pore size distribution of the aggregate could be correlated with field performance. Two of the problems that have been identified by KDOT engineers in Kansas concrete pavements are freeze-thaw damage and alkali-aggregate reaction. The main purpose of this phase of study was to develop a methodology to measure the pore size distribution of aggregates in concrete pavement cores using image analysis of scanning electron microscope images. A secondary purpose of the study was to determine if the aggregates used in the study were potentially AAR reactive.

1.3 Objectives and Scope of Study

The main objectives of this study were:

1. Develop a method for preparing and imaging samples of limestone coarse aggregates taken from concrete pavements for examination in the SEM.
2. Develop a computer program for image analysis of the limestone SEM images.

3. Use the sample preparation method and computer program developed to quantify the aggregate pore size distribution on concrete cores taken from two pavements with different field performance. The pavement performance has been kept from the researchers and labeled pavement A and B to make this a blind study.
4. Test the potential ASR reactivity of the aggregates in concrete cores taken from the same two concrete pavements using a method similar to the ASTM C 1260 accelerated mortar bar test (ASTM C 1260 2005).

Chapter 2: Methodology

2.1 Alkali-Silica Reaction

Potential for remaining alkali-silica reaction was determined by using a similar method to ASTM C 1260 and a method used in a previous study on the San Antonio "Y" structure in Texas. Two-inch diameter concrete cores were taken from the pavements for testing. Gauge studs were epoxied onto the core ends for measuring expansion. An eight-inch gauge length was used for the three cores tested from each pavement. The core lengths were measured before, during, and after being soaked in a 1N sodium hydroxide solution at 80°C for 11 weeks. A slightly lower soak solution-to-concrete ratio was used than what is required in the ASTM C 1260 test because of container size limitations (Williams 2005).

2.2 Aggregate Sample Preparation

The following procedure was developed for preparing aggregate samples from concrete cores for examination using a SEM:

1. The concrete core was cut in sections perpendicular to the core length using the Leco VC-50 precision saw shown in Figure 2.1. The cross sections were then trimmed to isolate individual aggregates. The selected aggregate was then sanded flat using 600 grit sandpaper and cleaned using compressed air.

FIGURE 2.1
Leco VC-50 Precision Saw Used to Remove Limestone Aggregates from Concrete Cores

2. The flattened end of the aggregate was placed on the bottom of a 1 ¼ inch diameter sample cup and placed in a vacuum chamber for epoxy impregnation. A two-part ultrathin epoxy supplied by Pace Technologies was added to the sample when the vacuum reached 27 inHg gauge pressure. The vacuum was released shortly after the epoxy covered the sample to keep the hardener from off-gassing. The epoxy impregnated sample was then allowed to cure for at least 24 hours at room temperature.
3. After removal of the sample from the sample cup, the top portion of the sample was flattened by saw cutting and grinding to ensure a uniform pressure on the sample surface during polishing.
4. The sample surface was then polished by hand using the following sandpapers:
    a. 320 grit for approximately 10 seconds
    b. 400 grit for approximately 30 seconds
    c. 600 grit for approximately 30 seconds
    d. 800 grit for approximately 15 seconds
    e. 1200 grit for approximately 15 seconds
5. The sample was checked to see if the aggregate sample had been exposed. If not, manual polishing was repeated starting with the 400 grit sandpaper.
6. The sample was cleaned in an isopropanol ultrasonic bath. The sample was then polished using the NANO 1000 grinder/polisher with the FEMTO 1000 automated polishing head (Pace Technologies) as shown in Figure 2.2. A propylene glycol drip was used for sample lubrication. Samples were cleaned between each automated polishing step in the isopropanol ultrasonic bath. The samples were polished at 200 rpm and 55 psi using the following polishing pads and diamond abrasive material:
    a. 9 μm diamond suspension on Texpan polishing pad for 2 hours
    b. 3 μm diamond suspension on Texpan polishing pad for 1.5 hours
    c. 1 μm diamond suspension on Atlantis polishing pad for 1.5 hours

FIGURE 2.2
NANO 1000 Grinder Polisher with FEMTO 1000 Automated Polishing Head Used in this Study

7. Carbon coat the sample to reduce charging during electron microscopy. Figure 2.3 shows a sample polished and carbon coated next to one that is polished but not yet carbon coated.

FIGURE 2.3
Epoxy Impregnated Aggregate after Polishing (Left) Next to an Epoxy Impregnated Aggregate Sample after Polishing and Carbon Coating (Right)

8. Image the sample in the SEM in backscattered electron mode. The FEI Nova NanoSEM 430 microscope located at the Kansas State University Microscopy Facility was used in this study. The images used for pore size distribution were taken using 600 times magnification. A custom made specimen mount shown in Figure 2.4 was used to keep the aggregate level in the microscope to eliminate the need for refocusing the SEM for each image.

FIGURE 2.4
Polished Aggregate Sample in Custom-Made Aluminum SEM Sample Mount

2.3 SEM Image Analysis

A program for quantifying the pore size distribution in limestone aggregate SEM images was written in C# (C Sharp). The software has built-in macro functionality, allowing the user to specify a series of image filters, treatments, analysis, and saving features that can be repeated on other images. Other program features include image histogram renormalization, median filter, binary thresholds, and pore detection. Figure 2.5 shows the software developed with an opened SEM image.

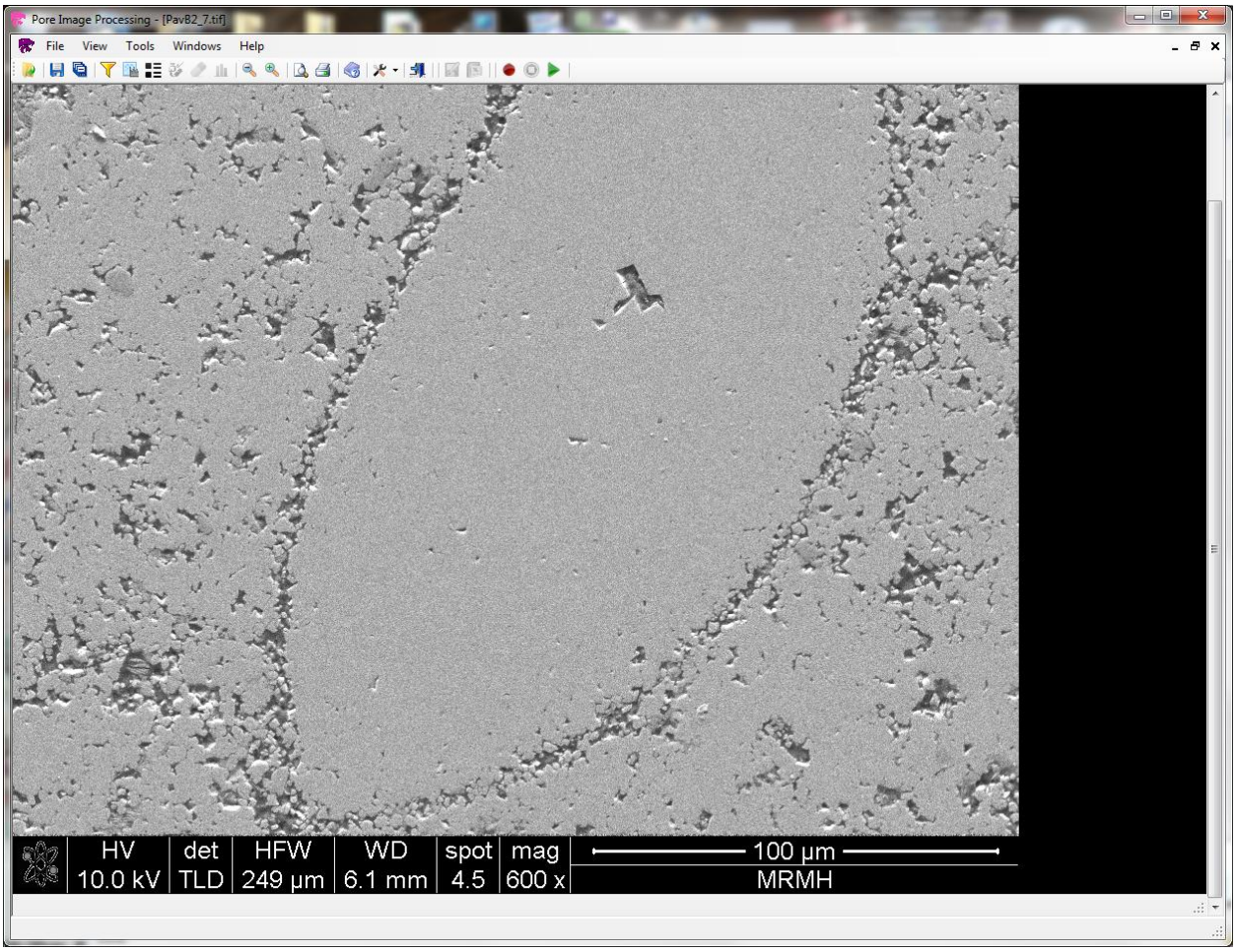

FIGURE 2.5
SEM Image Analysis Software Developed with an Open Aggregate SEM Image

The image processing routine used was to renormalize the image histogram, apply a median filter, apply a threshold based on pixel color to assign pixels as pores or limestone, and identify individual pores. Figure 2.6 shows the same image as shown in Figure 2.5 after the histogram normalization and application of a median filter. Figure 2.7 shows the same SEM image shown in Figure 2.5 and 2.6 after image histogram normalization, and threshold application. This is analogous to what is done in automatic hardened air void analysis, except with a higher magnification images taken using an SEM in backscattered electron (BSE) mode. The BSE mode detects electrons backscattered from the specimen, with high density materials giving higher counts of electrons. The epoxy-filled pores have a lower density than the limestone aggregate. This lower density makes the epoxy-filled pores look black in the SEM image in backscattered mode. After application of the grayscale threshold to separate out the black pores

from the lighter-colored solid limestone, individual pores were detected as shown in Figure 2.8. Once the pores were detected, the pixels in each pore were assigned to a layer based on how close the pixel was to the exterior of the pore. A pixel that was touching a limestone pixel would be assigned to layer one, whereas a pixel that had one pixel in between it and the edge of the pore would be assigned to layer two. The number of pixels in each layer, the total pore area, and maximum pore width were then calculated.

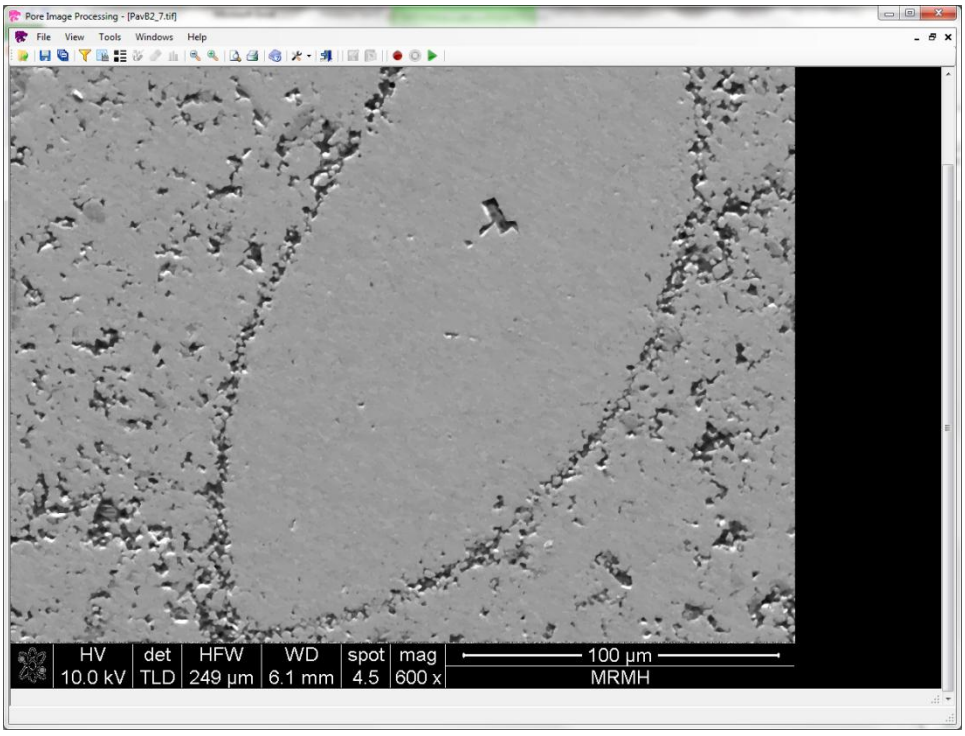

FIGURE 2.6
SEM Image after Histogram Normalization and Use of Median Filter

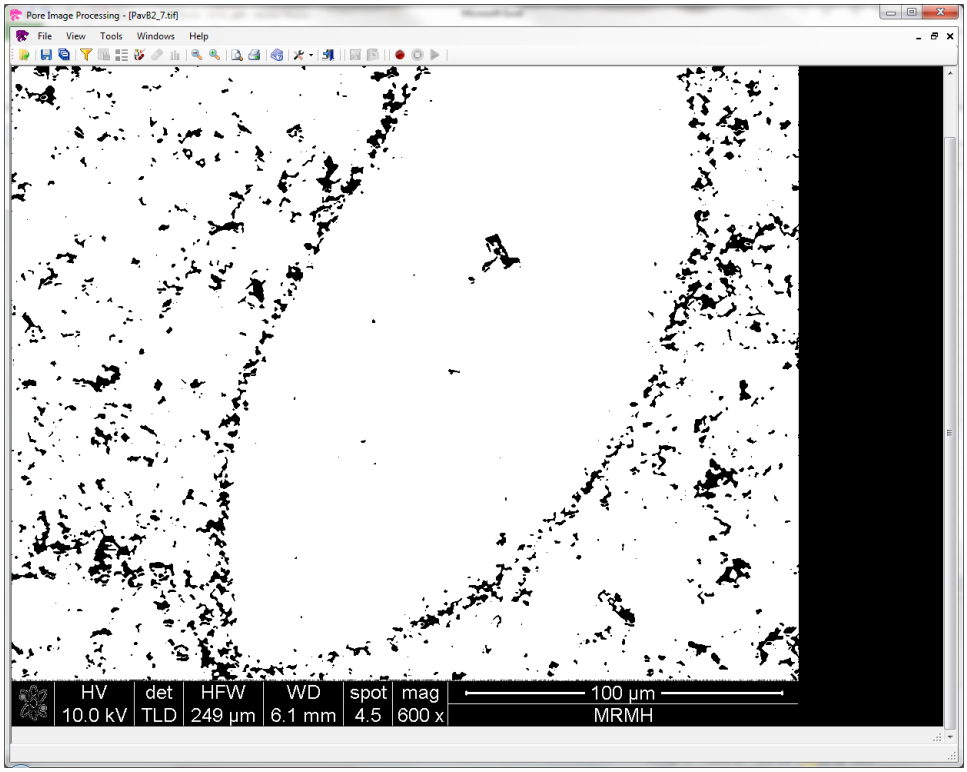

FIGURE 2.7
SEM Image after Pore Threshold Application

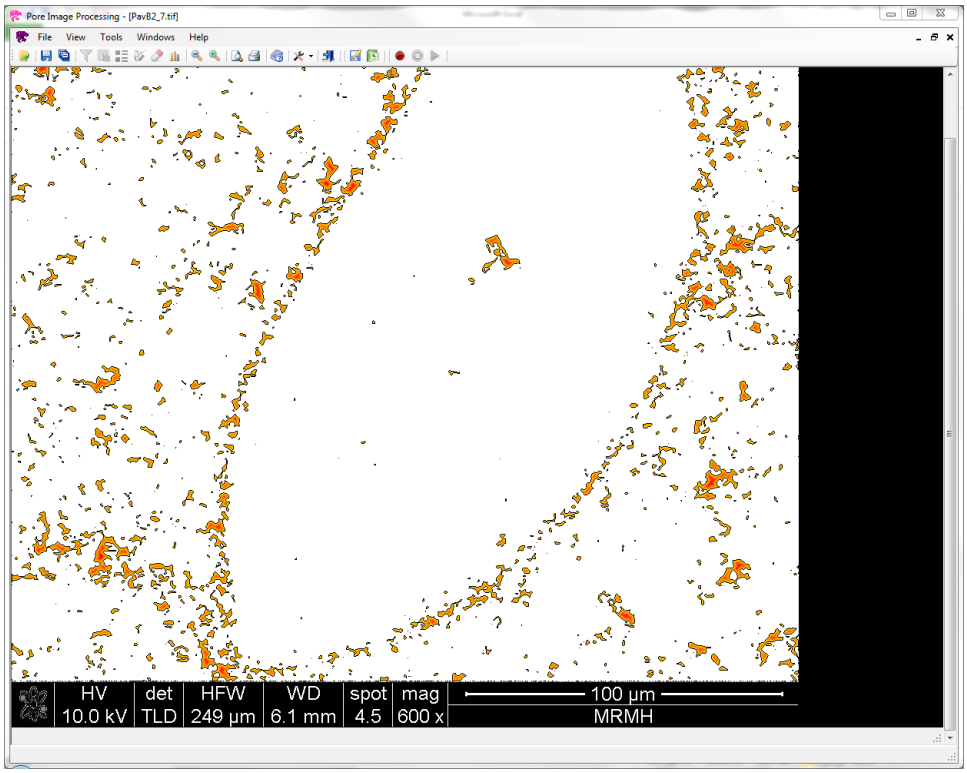

FIGURE 2.8
Pores Detected from the Same Image Shown in Figure 2.7

Chapter 3: Results and Discussion

3.1 Alkali-Aggregate Reaction Expansion

Testing for potential AAR expansion was performed by soaking three cores from each pavement in a 1N NaOH solution for 11 weeks. The average expansion for each pavement core set is shown in Figure 3.1. The small amount of expansion seen during the first week of soaking is less than what would normally be expected to occur with mortar bar specimens normally used in ASTM C 1260. This is because it takes twice as much time for alkalis to reach the center of the cores as it would the smaller mortar bar specimens that have a one inch by one inch cross section. Higher potential expansion seen in pavement B indicates that the aggregates used in pavement B have the potential for AAR reaction and deterioration given enough alkalis and water, which are much more prevalent at the joints.

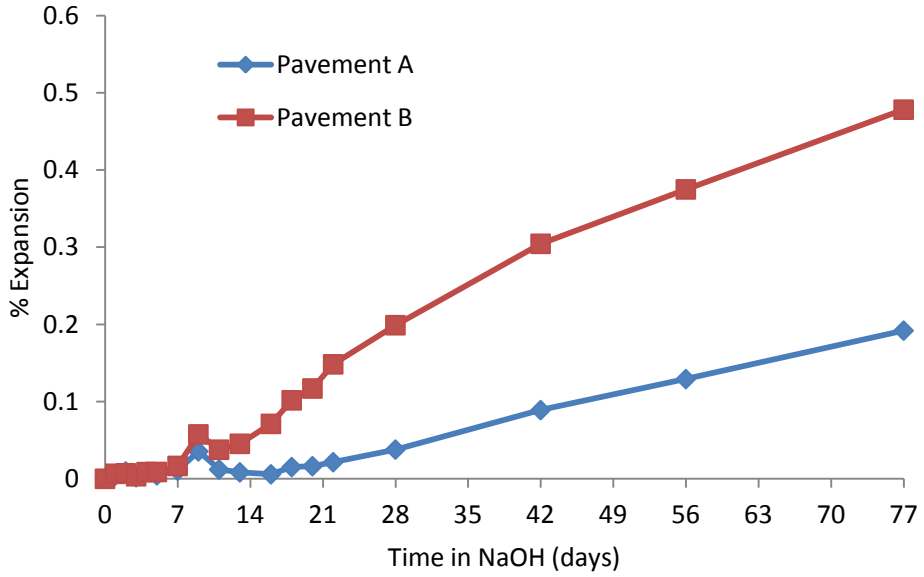

FIGURE 3.1
Expansion of Concrete Pavement Cores after Soaking in 1N NaOH Solution

3.2 Limestone Aggregate Pore Size Distribution

Approximately 50 SEM images for three aggregates from each pavement were taken for aggregate pore size distribution quantification. Pavement B showed a higher total aggregate porosity than pavement A as shown in Figure 3.2. Figure 3.2 gives the limestone aggregate pore size distribution as a function of the aggregate pore area, instead of the oft-used pore diameter. This is because aggregate pores are not spherical in shape, making the pore area a more accurate description of the pores. Figure 3.3 shows the number of pores per unit of area for each pore size. Aggregates in pavement B showed a much higher number of pores with an area between 0.1 and 1.5 μm^2. The number of aggregate pores with an area below 0.1 μm^2 was similar for both pavements; however this is because these pores were represented by only one pixel in the images. Smaller pores can be quantified in Phase II if desired by using a higher magnification which is recommended. This would, however, require taking more SEM images to image the same amount of aggregate area. The saw-tooth pattern shown in the aggregate pore size distribution in Figure 3.3 is likely an artifact of the discrete nature of pore areas and likely would be smoother when using a higher microscope magnification. The normalized cumulative pore size distribution for aggregate pores with an area less than 297.4 μm^2 (5000 pixels) was calculated by dividing the cumulative pore size distribution by the total area of the pores within this size, as shown in Figure 3.4. This showed that the pores in the aggregate from pavement A had a higher percentage of smaller pores than the aggregate from pavement B, although a smaller total amount.

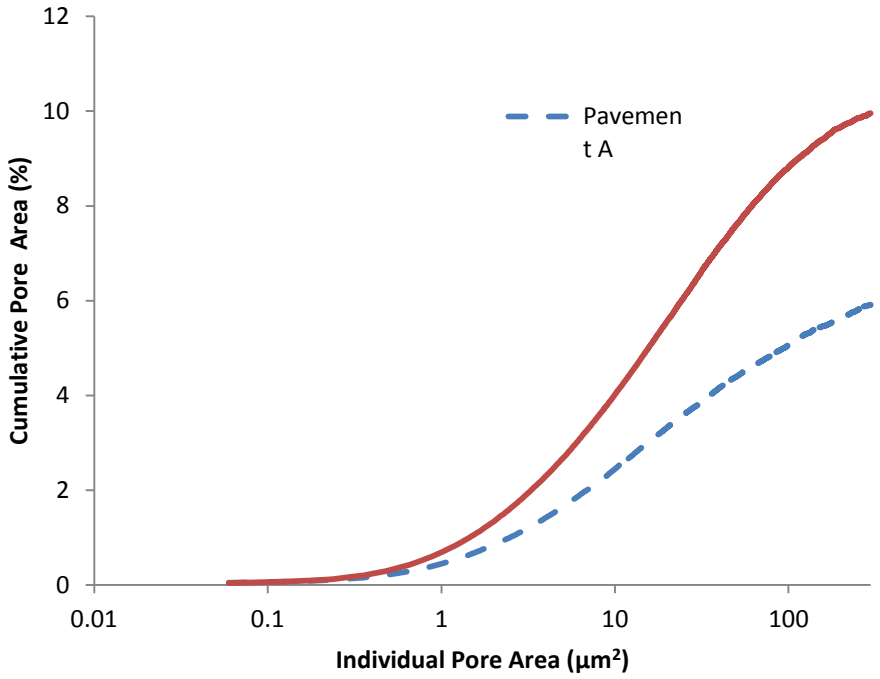

FIGURE 3.2
Limestone Aggregate Pore Size Distribution

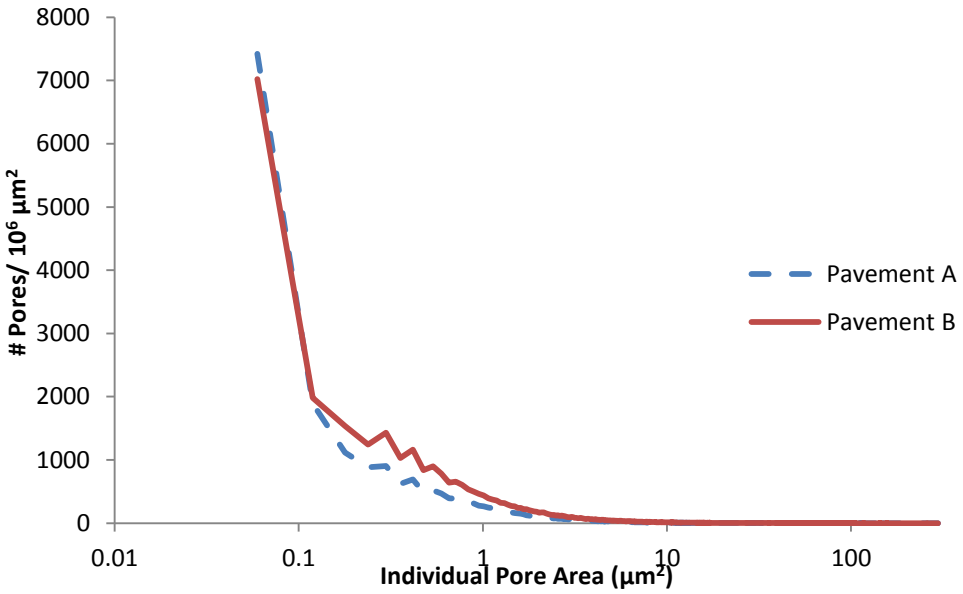

FIGURE 3.2
Number of Pores Measured for Each Pore Size

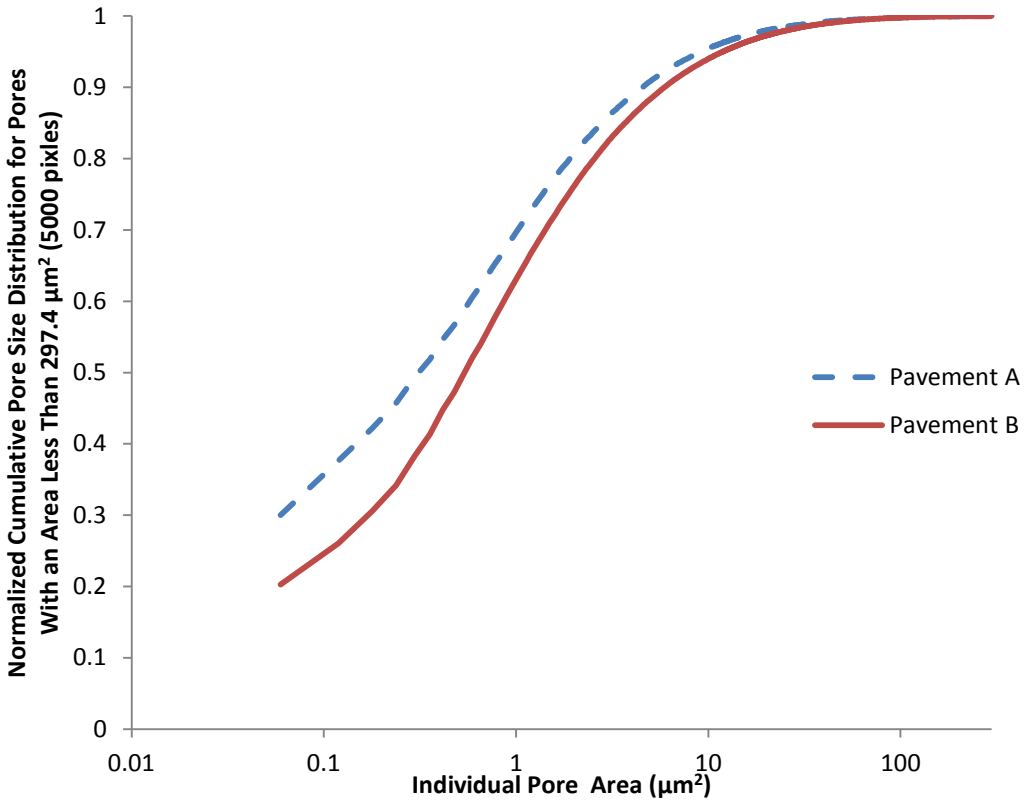

FIGURE 3.3
Pore Size Distribution Normalized by Total Pore Volume, Excluding Pores Larger than 297.4 µm^2

An analysis of the pore layer distribution seen in the pavements showed that pavement B had a higher amount of pores close to the solid limestone as shown in Figure 3.5. The smallest distance between pore edges seems to be an important factor governing both capillary action which governs water uptake and pore wall stresses from freezing and thawing (Hudec 1987). The area of pores found close to the pore wall measured by the layers in the SEM image analysis may be an indication of this aggregate property.

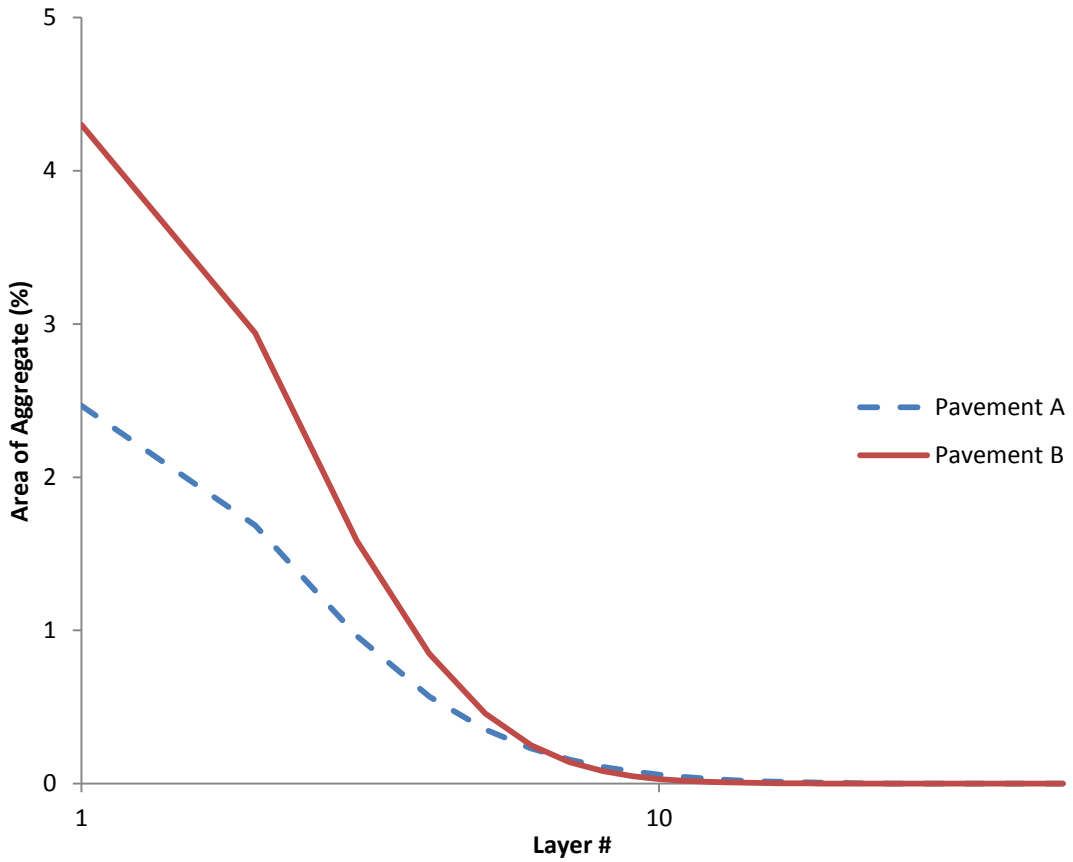

FIGURE 3.4
Pore Area by Layer from Solid Limestone

The SEM images also provided some insight into the aggregate and concrete properties besides the limestone coarse aggregate pore size distribution. The SEM images did not show entrained air voids filled with any ASR gel. Entrained air voids near the concrete pavement joint could have been filled with ettringite or ASR gel. SEM images near the joints should be taken to determine if the paste air void structure has been compromised. Figure 3.6 shows a large air void in the paste in pavement B near an aggregate, with cracks near the air void connecting aggregate pores. More research is needed to determine if aggregates sections near air voids in the paste show more or less susceptibility to freeze-thaw damage or if this cracking seen is just an artifact of the sample coring and saw cutting process.

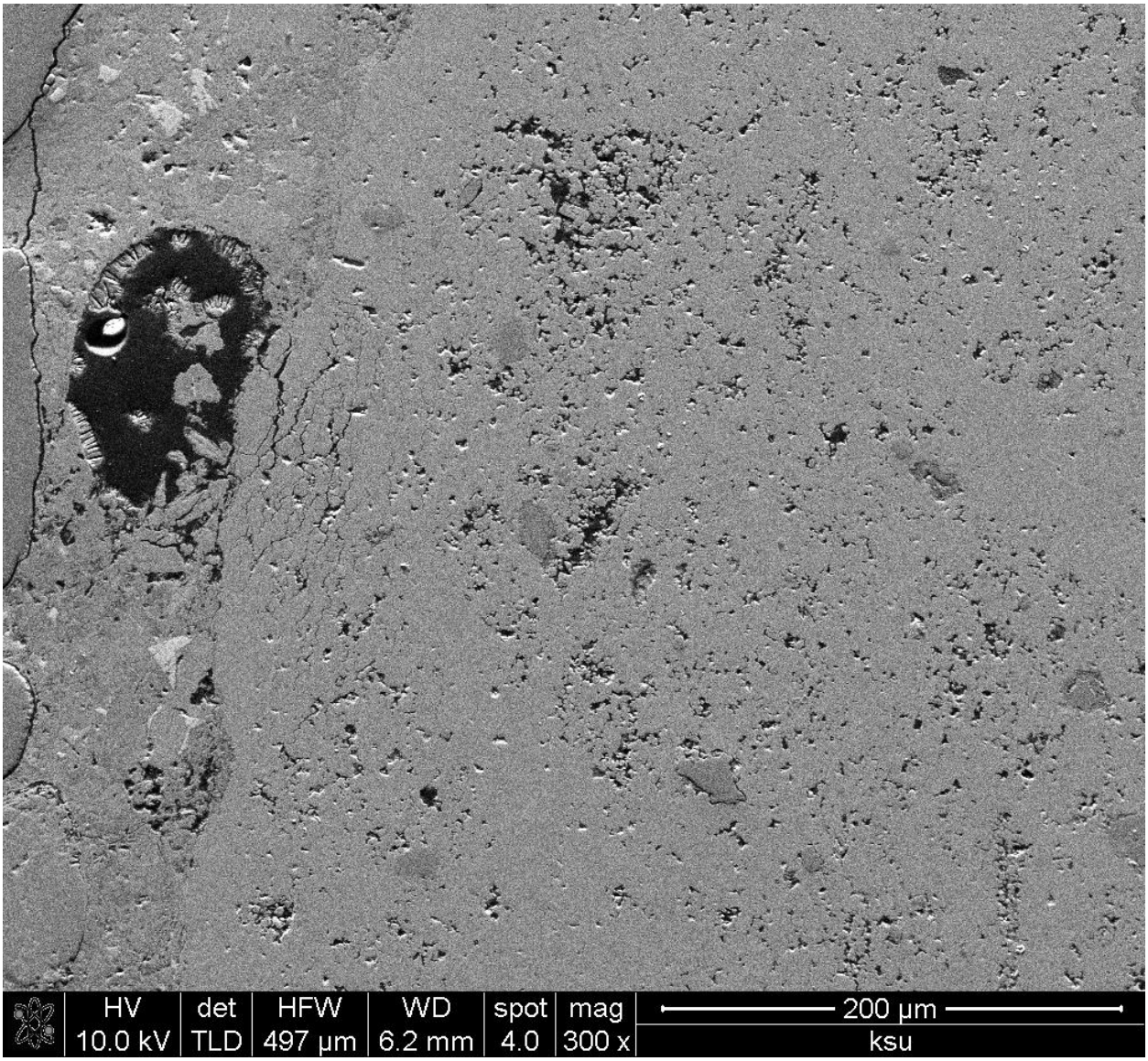

FIGURE 3.5
Microcracking Seen in the Aggregate from Pavement B near an Air Void

Chapter 4: Conclusions and Future Recommendations

4.1 Conclusions

Software for automating image analysis of aggregate pores in SEM images has been developed and used on samples taken from two different concrete pavements with different levels of field performance. A procedure has also been developed for sectioning, epoxy impregnating, and polishing limestone coarse aggregates from concrete cores for SEM image analysis. SEM image analysis showed that the aggregates from pavement B had a higher total porosity, and higher amount of small pores. Aggregates from pavement A however had a higher percentage of small pores (below 10 μm^2). The aggregates in pavement B showed a high potential for future AAR expansion given enough moisture and alkalis, which would be more available at the joints.

4.2 Future Recommendations

Based on the results of this Phase I project, the following recommendations for Phase II have been developed:

1. Use SEM image analysis to determine the aggregate pore size distribution on additional pavements with different performance histories to determine if aggregate pore size distribution can be used to predict the aggregate durability in concrete pavements.
2. Add a feature to the image analysis software to calculate pore size distribution based on the maximum pore width for each pore. The stresses generated inside an aggregate pore during freezing are a function of the pore size. Because real pores in aggregates are not spherical, it is believed that the maximum pore width could be a better indicator of freeze-thaw susceptibility than pore area as measured in the SEM images. For example, a long cylindrical pore with a small diameter could have a large volume, even though the stresses that would be generated during a freezing event would be higher than a spherical pore of equivalent volume but a larger diameter.
3. Use thermoporometry to determine the pore size distribution of limestone coarse aggregates. Thermoporometry determines the aggregate pore size distribution by

measuring the heat flows during water phase changes. In this test method, the saturated aggregate would be slowly frozen in a differential scanning calorimeter (DSC). The flow of heat away from the aggregate during freezing is measured in the test. An increase in the heat flow rate from the aggregate occurs during freezing in thermoporometry because of the latent heat of fusion. Water in smaller pores freezes at a lower temperature than water in larger pores, meaning that the peak heat flow rate for an aggregate with smaller pores would occur at a lower temperature.

4. Test pavement AAR potential by storing cores in sealed containers above water at 100°F similar to ASTM C-1293 instead of in 1N NaOH solution at 176°F. By measuring the core length changes above water at 100°F, the potential of the concrete pavement to undergo AAR expansion could be evaluated, rather than just the AAR potential of the aggregates in the concrete. This test method can evaluate if the aggregates are AAR reactive and whether or not the pavement alkalis are high enough to cause expansion in the concrete. Fortunately, because this test is similar to the ASTM C 1293 test method, it should show expansion when either alkali-carbonate reactive aggregates are used or alkali-silica reactive aggregates are used (Thomas, Fornier, and Folliard 2008). Petrographic analysis of concrete cores that show high levels of expansion would then show whether the expansion is from ASR or ACR. This test however takes a year to complete, which is why the more rapid test using a 1N NaOH soak solution was used in Phase I. The longer test based on ASTM C-1293 is also much better suited for testing the ACR form of expansion.

References

ASTM C 1260. 2005. "Standard Test Method for Potential Alkali Reactivity of Aggregates (Mortar-Bar Method)." West Conshohocken, Pennsylvania.

Dubberke, Wendell, and Vernon J. Marks. 1985. *The Effect of Deicing Salt on Aggregate Durability.* Transportaion Research Record.

Hudec, P. 1987. "Deterioration of Aggregates - The Underlying Causes." SP100-68. American Concrete Institute, 1325–1342.

Kaneuji, M., D. N. Winslow, and W. L. Dolch. 1980. "The Relationship between an Aggregate's Pore Size Distribution and Its Freeze Thaw Durability in Concrete." *Cement and Concrete Research* 10, no. 3: 433–441.

Niels, Thaulow, Jakobsen Ulla Hjorth, and Clark Boyd. 1996. "Composition of Alkali Silica Gel and Ettringite in Concrete Railroad Ties: SEM-EDX and X-Ray Diffraction Analyses." *Cement and Concrete Reseach* 26, no. 2: 309–318.

Pittenger, Robert, and Terry R. West. 1995. *Effects of Salt and Trace Minerals for Bituminous Pavements Literature Review, Information Gathering and Research Plan Development.* Interim Report, Joint Transportation Research Program.

Salcedo, Antonio Marco. 1984. *Identification of Frost Susceptible Aggregate and Their Use in Concrete or Bituminous Pavements.* Final Report, Joint Highway Research Project Report.

Shakoor, Abdul. 1982. *Evaluation of Methods for Predicting Durability Characteristics of Argillaceous Carbonate Aggregates for Highway Pavements.* Ph.D. Dissertation, Purdue University.

Thomas, M. D. A., B. Fournier, and K. J. Folliard. 2008. "Report on Determining the Reactivity of Concrete Aggregates and Selecting Appropriate Measures for Preventing Deleterious Expansion in New Concrete Construction." Final Report.

Williams, Stephanie Alayne. 2005. "Structures Affected by Premature Concrete Deterioration: Diagnosis and Assessment of Deterioration Mechanisms." Master's Thesis, the University of Texas at Austin.

AD ASTRA PER ASPERA

Kansas

Department of Transportation